Journal of Interfaces, Thin films, and Low dimensional systems 3 (2) Winter and Spring (2020) 287-295

The control of nonlinear optical properties in a doped asymmetric quantum dot by the spin-orbit coupling and external electric field

Scientific research paper

Parinaz Hosseinpour

Department of physics, Faculty of sciences, Sahand University of Technology, Tabriz 53318-17634, Iran

ARTICLE INFO

Article history:
Received 22 July 2020
Revised 6 November 2020
Accepted 16 December 2020
Available online 24 February 2021

Keywords:
Asymmetric quantum dot
Nonlinear optical properties
Rashba spin-orbit interaction
Gaussian impurity
Direction of electric field

ABSTRACT

The Rashba spin-orbit coupling in nanostructures is an important parameter that can affect their physical properties. Hence, it is demonstrated that the nonlinear optical properties of quantum dot such as second harmonic generation and optical rectification can be controlled by the Rashba spin-orbit coupling. Also, the effect of electric field and confinement potential strength on the nonlinear optical properties is examined. Our numerical study shows that magnitude of the second harmonic generation raises when the Rashba strength increases, while its peak position is not shifted. Moreover, the optical rectification of doped asymmetric quantum dot shifts to higher energies when the electric field enhances.

1 Introduction

Nonlinear optical phenomena are "nonlinear" in the sense that they occur when the response of a material system to an applied optical field depends in a nonlinear manner on the strength of the optical field. The nonlinear response of the material's polarization to the electric field of incident light causes the nonlinear behavior of the environment. In fact, nonlinear optical properties describe the interaction of light with material, in which the material's optical response is highly dependent on the incident light. For example, second-harmonic generation (SHG) occurs as a result of the part of the atomic response that scales quadratically with the strength of the applied optical field. Consequently, the intensity of the light generated at the second-harmonic frequency tends to increase as the square of the intensity of the applied laser light. Furthermore, the optical rectification can takes place in the nonlinear environment, in which a static electric field is created across the nonlinear structures.

Among the various structures, nonlinearity of the semiconductor quantum dot (QD) is very remarkable.

*Corresponding author.
Email address: Phosseinpour@sut.ac.ir
DOI: 10.22051/jitl.2020.32337.1041

This quantum structure has some advantages such as large transition matrix elements between different quantum levels and the energy spectrum similar to the atomic or molecular systems [1]. Also, QDs can be an ideal candidate for light encoding due to their narrow emission spectrum. The possibility of manipulation of these structures implies them to be used in solar cell transistors, LEDs, medical imaging, and quantum computing. Adding the impurity atoms is one way to manipulate the quantum dots and control their optical properties [2-7]. Among the nonlinear optical properties in nanostructures, the SHG and nonlinear optical rectification (NOR) have attracted a lot of attention [8-20]. These quantities have been widely studied in quantum wells. For example, Qiucheng, et. al studied the second-harmonic generation in a quantum well by solving the Schrödinger equation with position-dependent mass [13]. Also, the SHG has been investigated in quantum wells under applied electric and magnetic fields [14]. Martínez. et. al investigated the nonlinear optical properties in a double quantum well [15]. Cakir et. al. and Karabulut et. al. investigated the impurity effect on the linear and nonlinear optical properties of a spherical QD [16]. Rezaei et. al. discussed the effects of hydogenic impurity confined in a quantum dot under the external perturbations on the linear and third order nonlinear optical properties [17]. Chen et. al. calculated the nonlinear optical rectification of impurity with ellipsoidal confinement potential in the presence of applied electric field [18]. Yilmaz investigated the binding energies of ground state, excited states, OR and oscillator strength in a spherical quantum dot having parabolic confinement with an off-center hydrogenic impurity without the magnetic field and under an applied electric field [19]. Shojaei and Soltani-Vala theoretically studied the effect of combined electric and magnetic field on OR in a two dimensional disk-like quantum dot with parabolic confinement potential and hydrogenic impurity [20]. All studies have shown that external factors such as impurities, electric and magnetic fields, pressure and temperature can change the nonlinear optical properties of nanostructures. But the effect of Rashba spin-orbit coupling (SOC) and electric field (magnitude and direction) in a doped asymmetric quantum dot with Gaussian impurity on the nonlinear properties has not been studied in more detail. Therefore, in this paper, an asymmetric quantum dot is assumed and all the calculations are done in the framework of effective mass approximation and the formulation of the density matrix. In fact, we show that the different SOC strengths, direction, and magnitude of electric field can be used to control the optical response of quantum dots for practical applications such as double-frequency light production (SHG) and optical rectification. In my pervious paper, the role of Rashba spin-orbit interaction in the thermal properties of a doped quantum dot has been studied [21].

2 Model and theory

In general, dependency of the polarization of a material on the strength of an applied optical field shows the nonlinear behavior of structures. In the case of conventional (i.e., linear) structures, the induced polarization depends linearly on the electric field strength. But, in nonlinear materials, the optical response can often be described by expressing the polarization as a power series in the field strength. So that, the coefficient of the square of field represents the second-order optical propFerties. The second-order polarization consists of a contribution at zero frequency and a contribution at frequency 2ω. The latter contribution can lead to the generation of radiation at the second-harmonic frequency. This is while the first contribution does not lead to the generation of electromagnetic radiation; it leads to a process known as optical rectification, in which a static electric field is created across the nonlinear material [22-24]. The second-harmonic generation ($\chi^{(2)}_{2\omega}$) and optical rectification ($\chi(\omega)$) can be calculated as follows [25, 26]:

$$\chi^{(2)}_{2\omega} = \frac{e^3 N M_{01} M_{12} M_{20}}{\varepsilon_0 h^2 (\omega - \omega_{10} + i\Gamma_{10})(2\omega - \omega_{20} + i\Gamma_{20})}, \qquad (1a)$$

$$\chi(\omega) = \frac{4e^3 N M_{01}^2 \delta_{01}}{\varepsilon_0 h^2} \times \frac{\omega_{10}^2 \left(1 + \frac{T_1}{T_2}\right) + (\omega^2 + \frac{1}{T_2^2})\left(\frac{T_1}{T_2} - 1\right)}{\left[(\omega_{10} - \omega)^2 + \frac{1}{T_2^2}\right]\left[(\omega_{10} + \omega)^2 + \frac{1}{T_2^2}\right]}, \qquad (1b)$$

where, $\hbar\omega$, N, ε_0, $\frac{1}{\Gamma_{10}} = \frac{1}{\Gamma_{20}} = \frac{1}{\Gamma}$, T_1, and T_2 are the incident photon energy, the carrier density in the QD, the permittivity of vacuum, the relaxation time,

longitudinal and the transverse relaxation times, respectively. The transition matrix elements (M_{ij}) and δ_{01} are defined as $M_{ij} = |\langle \phi_i | e \cdot r | \phi_j \rangle|$ and $\delta_{01} = |\langle \phi_0 | e \cdot r | \phi_0 \rangle - \langle \phi_1 | e \cdot r | \phi_1 \rangle|$ where i, j=0, 1, 2. 0, 1 and 2 refer to ground, first and second excited states, respectively while "r" represents the incident light polarization. From Eq. (1a), it is seen that the second-harmonic generation has two maximum values whose positions are strongly dependent on the transition energy between the ground and the first excited state ($\omega_{10} = E_1 - E_0/\hbar$) and the transition between the ground and the second excited state ($\omega_{20} = E_2 - E_0/\hbar$). Also, the maximum values of the SHG and OR were determined by the product of the transition matrix elements between the aforementioned three states ($M_{01}M_{12}M_{20}$) and geometric factor (GF) ($M_{01}^2\delta_{01}$), respectively.

In this work, the quantum dot is a nanometer-scale blob of narrow-bandgap semiconductor (i.e. InAs), surrounded by a wider-bandgap semiconductor. This structure is assumed as a disk in two-dimensional x-y plane with assuming that the z-direction can be considered zero. The confinement potential of QD becomes asymmetric harmonic oscillator potential that means the oscillator strength in two dimensions of 'x' and 'y' ($\hbar\omega_{0x}$ and $\hbar\omega_{0y}$) is different. Moreover, this disk-like QD is doped with adding the impurity atoms whose potential becomes Gaussian. In order to obtain the energy levels (E) and wave-functions (Ψ), The Schrodinger equation of one electron in a doped QD ($H\Psi = E\Psi$) should be solved. Within the framework of effective mass approximation, the Hamiltonian (H) of a doped QD in the presence of external electric field (F) with including the Rashba SOC is given by

$$H = \frac{1}{2m^*}\left(\vec{p} - \frac{e}{c}\vec{A}\right)^2 + \frac{1}{2}m^*\left[(\omega]\right]_{0x}^2 x^2 + \omega_{0y}^2 y^2\right) + eFx\cos\varphi + V^{imp}(x,y) + \frac{\alpha_R}{\hbar}\left[\sigma \times \left(\vec{p} - \frac{e}{c}\vec{A}\right)\right]_z, \quad (2)$$

where the first and second terms are the kinetic energy and asymmetric harmonic oscillator confinement potential of carriers in QD, respectively. With the advances in synthesizing quantum dots, the different shapes of dots can be modeled [27-31]. Hence, various types of confinement potentials have been theoretically proposed and investigated that among them, the parabolic potential can be appropriate. ($\vec{p} - \frac{e}{c}\vec{A}$) is the canonical momentum where the vector potential ($\vec{A}$) is given as $\vec{A} = \frac{B}{2}(-y,\ x, 0)$ (B is the magnetic field). 'F' and 'φ' are the magnitude and direction (angle between the applied electric field and x-axis) of the applied electric field. The fourth term ($V^{imp}(x,y) = V_0 e^{-[(x-x_0)^2+(y-y_0)^2]/d^2}$) is the Gaussian impurity potential; where V_0 is the impurity strength with $V_0 > 0$ ($V_0 < 0$) for a repulsive (an attractive) impurity and "d" is an impurity parameter that determines the amount of spatial distribution of the impurity [32]. Also, (x_0, y_0) denotes position of the impurity center in the quantum dot. The last term is Rashba SOC where α_R is the Rashba coupling coefficient which can be controlled by the gate voltage applied in the z-direction. Spin-orbit interaction is one of the most essential interactions in nanostructures. SOC is described by two different sources of potential asymmetries: (i) the first one arises from the bulk inversion asymmetry, in which the crystal lacks a center of space inversion. The spin–orbit coupling caused by this inversion asymmetry is known as a Dresselhaus interaction [33], (ii) the second one arises from the structural inversion asymmetry known as a Rashba interaction [34] which is only possible in low dimensional systems where the semiconductor loses the symmetry in the growth direction.

The electronic structure of doped QD is obtained by solving the matrix form of the Hamiltonian presented by Eq. (2) within the exact diagonalization method by expanding the matrix in basis of the eigen-function of the confined electron in two-dimensional asymmetric oscillator potential

$$\Psi_{n,m}(x,y) = \sum_n \sum_m C_{nm}\varphi_n(x)\varphi_m(y),$$

$$\varphi_n(x) = \frac{1}{\sqrt{2^n n!}}\left(\frac{\alpha_x}{\sqrt{\pi}}\right)^{\frac{1}{2}} e^{-\frac{\alpha_x^2 x^2}{2}} H_n(\alpha_x x),\ \alpha_x = \left(\frac{m^*\omega_{0x}}{\hbar}\right)^{1/2},$$

$$\varphi_m(y) = \frac{1}{\sqrt{2^m m!}}\left(\frac{\alpha_y}{\sqrt{\pi}}\right)^{\frac{1}{2}} e^{-\frac{\alpha_y^2 y^2}{2}} H_m(\alpha_y y),$$

with $\alpha_y = (\frac{m^*\omega_{0y}}{\hbar})^{1/2}$, C_{nm} are the variational parameters and H_n is the nth-order Hermite polynomial). With replacement of the operator forms of $\hat{x}$, $\hat{y}$, $\widehat{p_x}$ and $\widehat{p_x}$ in the Hamiltonian

represented by Eq. (2) using the annihilation ($a_x = \sqrt{\frac{m^*\omega_{0x}}{2\hbar}}(\hat{x} + \frac{i}{m^*\omega_{0x}}\widehat{p_x})$ and $a_y = \sqrt{\frac{m^*\omega_{0y}}{2\hbar}}(\hat{y} + \frac{i}{m^*\omega_{0y}}\widehat{p_y})$) and creation operator ($a_x^+ = \sqrt{\frac{m^*\omega_{0x}}{2\hbar}}(\hat{x} - \frac{i}{m^*\omega_{0x}}\widehat{p_x})$ and $a_y^+ = \sqrt{\frac{m^*\omega_{0y}}{2\hbar}}(\hat{y} - \frac{i}{m^*\omega_{0y}}\widehat{p_y})$), the matrix elements of Hamiltonian ($\langle n, m|H|n', m'\rangle$) are given by

$$\begin{aligned}
&\langle n,m|H|n',m'\rangle \\
&= \left\langle n,m\left|\hbar\omega_{0x}\left(\frac{1}{2}+a_x^\dagger a_x\right)\right|n',m'\right\rangle \\
&+ \left\langle n,m\left|\hbar\omega_{0y}\left(\frac{1}{2}+a_y^\dagger a_y\right)\right|n',m'\right\rangle \\
&+ \left\langle n,m\left|\frac{\alpha_R\sqrt{2m^*\hbar\omega_{0x}}}{4\hbar}\left(a_x\sigma_+ + a_x^\dagger\sigma_- - a_x\sigma_-\right.\right.\right. \\
&\left.\left.\left. - a_x^\dagger\sigma_+\right)\right|n',m'\right\rangle \\
&+ \left\langle n,m\left|\frac{i\alpha_R\sqrt{2m^*\hbar\omega_{0y}}}{4\hbar}\left(a_y^\dagger\sigma_+ - a_y\sigma_- + a_y^\dagger\sigma_-\right.\right.\right. \\
&\left.\left.\left. - a_y\sigma_+\right)\right|n',m'\right\rangle \\
&+ \left\langle n,m\left|\frac{eF\cos\varphi}{2}\sqrt{\frac{2\hbar}{m^*\omega_{0x}}}(a_x + a_x^\dagger)\right|n',m'\right\rangle \\
&+ \langle n,m|V^{imp}|n',m'\rangle. \qquad (3)
\end{aligned}$$

where $\sigma_\pm = \sigma_x \pm i\sigma_y$ and the matrix elements of V^{imp} are given by [35] as

$$(V^{imp})_{n,m;n',m'} = D_x D_y \sum_{k=0}^{\min(n,n')} \sum_{l=0}^{\min(m,m')} f(k,n,n')\, g(l,m,m'), \qquad (4)$$

where $D_x = A\lambda_x\pi^{1/2}/\delta_x$, $f(k,n,n') = 2^k\, k!\; {}^nC_k\; {}^{n'}C_k\,(1-\alpha_x^{*2})^{\frac{n+n'}{2}-k}\, H_{n+n'-2k}(\alpha_1\rho_x)$, $D_y = B\lambda_y\pi^{1/2}/\delta_y$ and $g(l,m,m') = 2^l\, l!\; {}^mC_l\; {}^{m'}C_l\,(1-\alpha_y^{*2})^{\frac{m+m'}{2}-l}\, H_{m+m'-2l}(\beta_1\rho_y)$

with $A = \alpha/(2^{n+n'}\, n!\; n'!\,\pi)^{1/2}$, $\alpha_x^* = \alpha/\delta_x$, $\lambda_x = \exp[-x_0^2(\delta_x^2 - \frac{1}{d^2})/d^2\delta_x^2]$, $\delta_x^2 = \alpha_x^2 + \frac{1}{d^2}$, $\rho_x = x_0/d^2\delta_x$, $\alpha_1 = \alpha_x^*/(1-\alpha_x^{*2})^{1/2}$, $\alpha_y^* = \alpha/\delta_y$ $B = \alpha/(2^{m+m'}\, m!\; m'!\,\pi)^{1/2}$, $\delta_y^2 = \alpha_y^2 + \frac{1}{d^2}$, $\lambda_y = \exp\left[-y_0^2\left(\delta_y^2 - \frac{1}{d^2}\right)/d^2\delta_y^2\right]$, $\rho_y = y_0/d^2\delta_y$, $\beta_1 = \alpha_y^*/(1-\alpha_y^{*2})^{1/2}$, and ${}^nC_k = \frac{n!}{(n-k)!k!}$.

In our numerical calculations, eigenvalues of Hamiltonian matrix converge are for dimension of 28×28. Therefore, energy eigen-values of a doped QD can be obtained within the exact diagonalization method.

3 Results and Discussion

In this section, the results of numerical calculations are shown for the InAs quantum dot. The values of the parameters in this calculation are: $m^* = 0.023m_e$ (m_e is the electron mass), $\Gamma = 0.5 \times 10^{12}\ s^{-1}$, $N = 3.59 \times 10^{22}\ m^{-3}$, $T_1 = 1$ ps, $T_2 = 2$ ps.

Firstly, we report the effect of the Rashba coupling factor on the nonlinear optical properties (SHG and OR) of a doped asymmetric QD. In order to provoke a structure to exhibit nonzero optical rectification response, the rotational symmetry must be broken. To achieve this aim in nanostructures, simultaneous presence of impurity and external electric field is essential. For this reason, the effect of α_R on the nonlinear optical properties of a doped asymmetric QD with on-center Gaussian impurity under the electric field ($F = 0.5\ ^{kV}/_{cm}$) has been investigated. In Figs. 1 and 2, SHG and OR of a doped asymmetric QD with confinement potential of $\hbar\omega_{0x} = 3$ meV, $\hbar\omega_{0y} = 4$ meV and repulsive (attractive) impurity as a function of the incident photon energy with x-direction polarization for various Rashba spin-orbit coupling strength has been demonstrated, respectively.

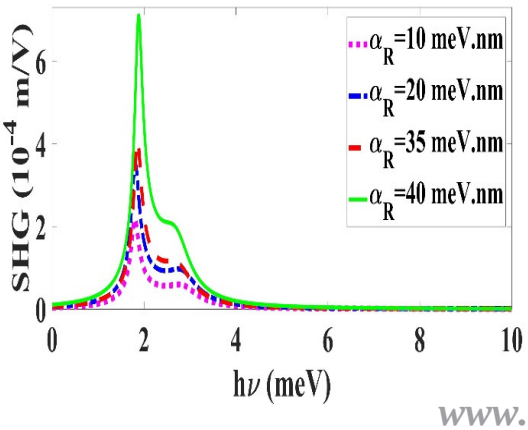

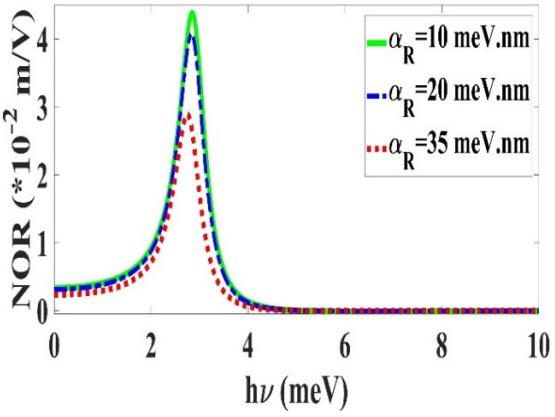

Figure 1. The top panel shows the second harmonic generation and the bottom panel shows the optical rectification of a doped asymmetric QD with on-center repulsive impurity (V_0= 32 meV, d=5 nm) as a function of the incident photon energy with x-direction polarization for various Rashba spin-orbit coupling strength at fixed electric field $\boldsymbol{F = 0.5\ ^{kV}/_{cm}}$.

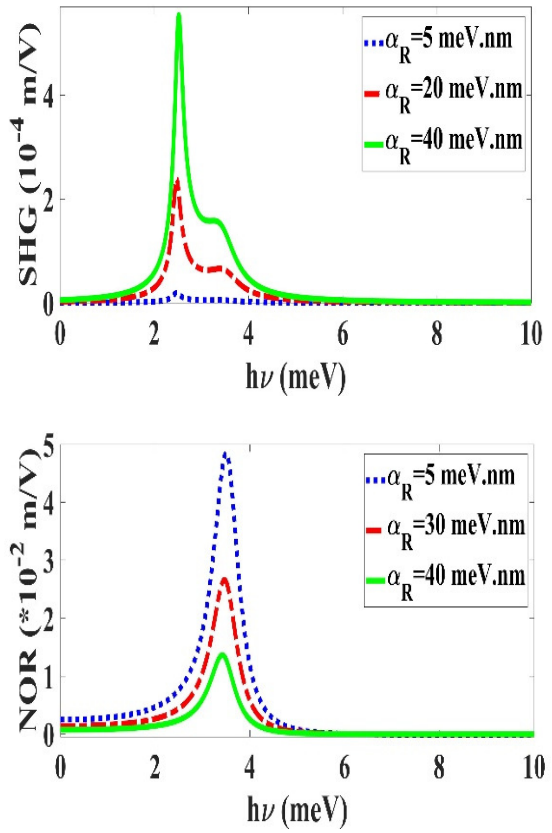

Figure 2. The top panel shows the second harmonic generation and the bottom panel shows the optical rectification of a doped asymmetric QD with on-center attractive impurity (V_0= -32 meV, d=5 nm) as a function of the incident photon energy with x-direction polarization for various Rashba spin-orbit coupling strength at fixed electric field $\boldsymbol{F = 0.5\ ^{kV}/_{cm}}$.

By increasing the Rashba coupling, the value of SHG increases while the peak position does not change as observed in the top panels of Figs. 1 and 2. The reason for this behavior is that by including the spin-orbit coupling, all energy levels of QD decrease. Then, the overlapping of wave-functions ($M_{01}M_{12}M_{20}$) and SHG magnitude enhance. It should be noted that the behavior of QD energy levels versus spin-orbit coupling strength has already examined in our pervious paper [36]. On the other hand, the effect of Rashba coupling on the optical rectification of a doped asymmetric QD has been shown in the bottom panels of Figs. 1 and 2 for repulsive and attractive impurity, respectively. It is clear that the enhancement of the spin-orbit coupling decreases the light rectification. This behavior is related to the reduction of the geometric factor (GF) versus α_R, which can be seen in Fig. 3.

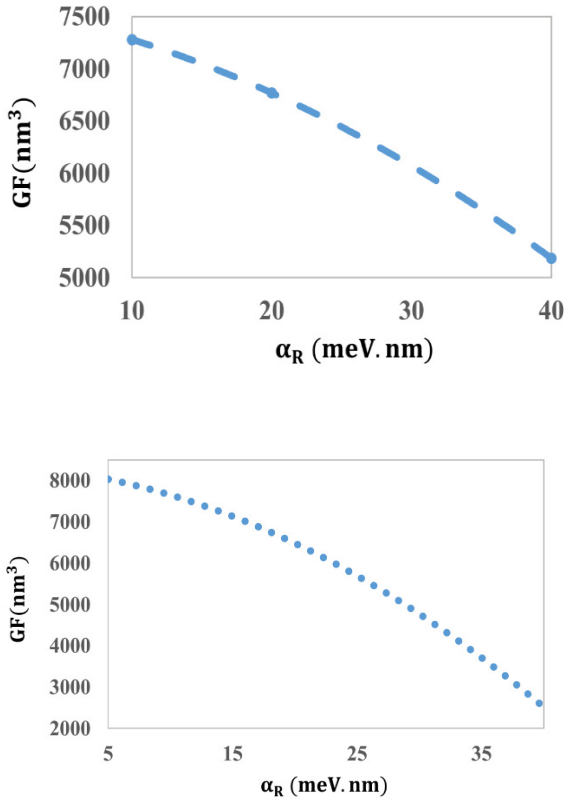

Figure 3. The geometric factor (GF) of a doped asymmetric QD with on-center (top panel) repulsive (V0= 32 meV, d=5 nm) and (bottom panel) attractive (V0= -32 meV, d=5 nm) impurity versus Rashba spin-orbit coupling strength.

In the following, effect of the confinement energy ratio in a two dimensional plane of QD ($\hbar\omega_{0x}/\hbar\omega_{0y}$)

(degree of QD anisotropy) on SHG and OR is studied as presented in the top and middle panels of Fig. 4. It is expected that the transition matrix elements ($M_{ij} = |\langle \phi_i|x|\phi_j\rangle|$) for strong confinement energy decrease due to more localized wave-function. Therefore, magnitude of SHG and OR decrease when the degree of QD anisotropy increases. Also, it is clear that degree of QD anisotropy leads to peak position blue-shifts. The reason for this behavior is that the transition energy between the ground and first excited states ($\Delta E_{10} = E_1 - E_0$) increases when the carriers are confined strongly as illustrated in the bottom panel of Fig. 4.

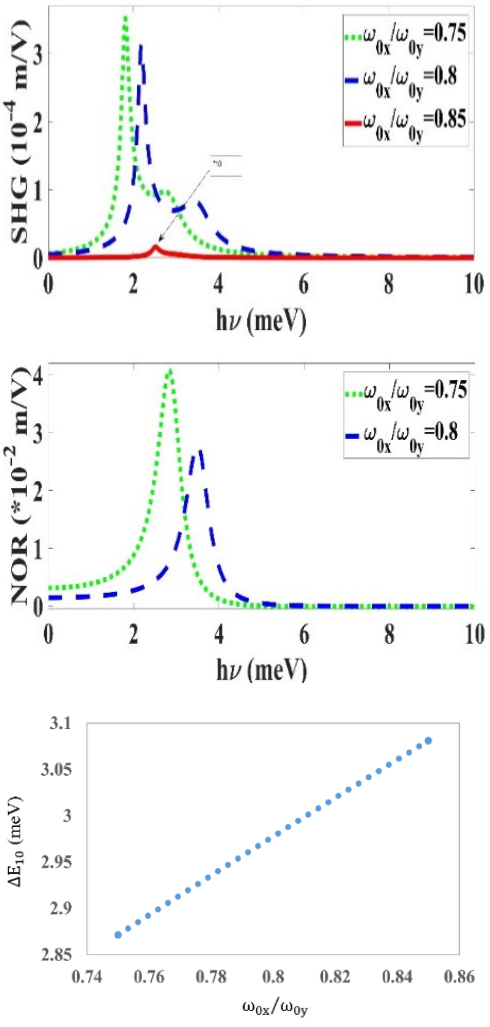

Figure 4. The top panel shows the second harmonic generation, the middle panel shows the optical rectification, and bottom panel shows the transition energy of a doped asymmetric QD with on-center repulsive impurity (V_0= 32 meV, d=5 nm) as a function of the incident photon energy with x-direction polarization for various ω_{0x}/ω_{0y} at fixed electric field and Rashba coupling (F = 0.5 kV/cm and $\alpha_R = 20$ meV.nm).

In Fig. 5, we have investigated SHG and NOR of a doped asymmetric QD for various electric fields with ϕ =0°, respectively. The top panel of Fig. 5 depicts that by applying the external electric field, energy levels reduce and wave-function overlapping increases. Then, magnitude of SHG enhances. On the other hand, at strong electric fields, additional confinement of electron in QD occurs, then wave-functions are localized and GF reduces. Also, enhancement of the electric field leads to increase of the transition energy between levels. Therefore, position of NOR peak shifts to higher frequencies (blue-shift).

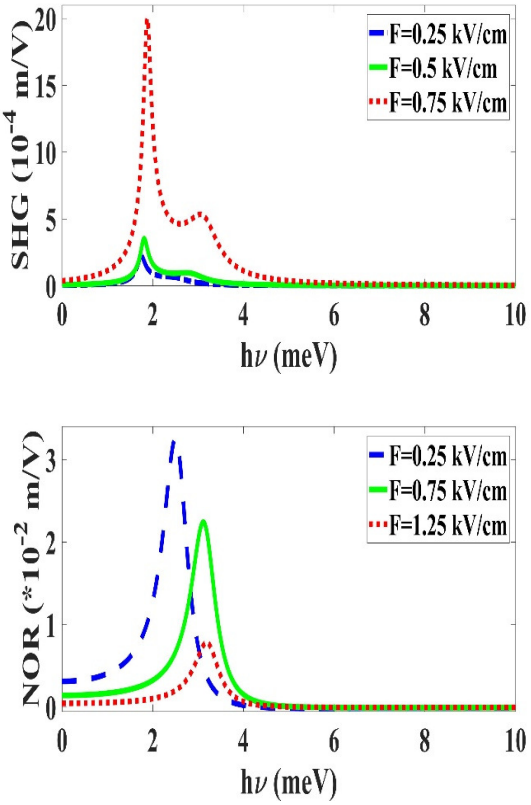

Figure 5. The top Panel shows the second harmonic generation, the bottom panel shows the optical rectification of a doped asymmetric QD with on-center repulsive impurity (V0=32 meV, d=5 nm) as a function of the incident photon energy with x-direction polarization for various electric fields at fixed $\alpha_R = 20$ meV.nm.

Moreover, the effect of electric field direction (angle between applied electric field and horizontal axis) on SHG and NOR has been represented in Fig. 6.

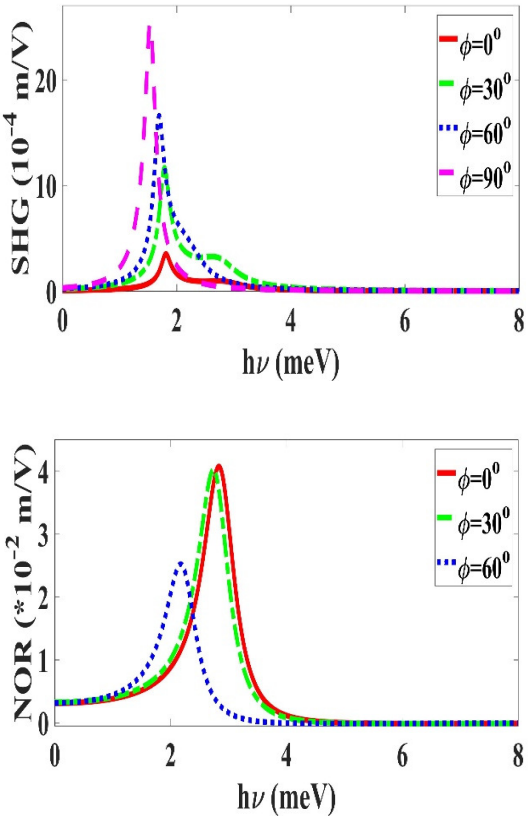

Figure 6. The top panel shows the second harmonic generation, the bottom panel shows the optical rectification of a doped asymmetric QD with on-center repulsive impurity (V_0=32 meV, d=5 nm) as a function of the incident photon energy with x-direction polarization for various direction of applied electric field at the fixed magnitude of electric field and Rashba coupling (F = 0.5 $^{kV}/_{cm}$ and α_R = 20 meV. nm).

From the top panel of Fig. 6 we observe that the SHG magnitude increases as the angle increases from 0° to 90°. According to Eq. (2), the term of "F.cosφ" has the role of effective electric field, therefore with increasing the angle from 0° to 90°, the effective electric field decreases and the confinement of carrier reduces; then enhancement of wave-function overlapping as well as the SHG magnitude occurs, while reduction of the effective electric field causes the geometric factor to decrease before optical rectification reduces.

4 Conclusions

To summarize, we studied the changes of nonlinear optical properties such as SHG and NOR of a doped asymmetric QD with repulsive Gaussian impurity versus strength of Rashba spin-orbit coupling, confinement potential, and applied electric field. Our numerical calculations showed that SHG and NOR have the tuning capability by changing these parameters; so that the maximum value of SHG is obtained by increasing the spin-orbit coupling and electric field. On the other hand, the effect of confinement strength ratio in disk-plane of QD on the nonlinear optical properties of QD was examined. Also, influence of the applied electric field direction on SHG and OR has been investigated. In fact, have shown that the Rashba strength is the key parameter to control nonlinear optical properties of QD without shifting the peak position. While enhancement of the confinement energy leads to the position of SHG and NOR peak shifts toward higher energy as the magnitude of optical rectification decreases.

References

[1] V. Vijit, P. S. Nautiyal, "Second harmonic generation in a disk shaped quantum dot in the presence of spin-orbit interaction." Physics Letters A, **382** (2018) 2061.

[2] A. S. Sachrajda, Y. Feng, R. P. Taylor, G. Kirczenow, L. Henning, J. Z. P. Wang and P. T. Coleridge, "Magneto-conductance of a nanoscale anti-dot." Physical Review B, 50 (1994) 10856.

[3] V. Margulis, A.V. Shorokhov, "Hybrid–impurity resonances in anisotropic quantum dots." Physica E, 41 (2009) 483.

[4] V. D. Jovanovic, D. Indjin, N. Vukmirovic, Z. Lkonic, P. Harrison, E. H. Linfield, H. Page, X. Marcadet, C. Sirtori, C. Worall, H. A. Beere and D. A. Ritchie, "Mechanisms of dynamic range limitations in GaAs⁄AlGaAs quantum-cascade lasers: Influence of injector doping." Applied Physics Letter, 86 (2005) 211117.

[5] E. Mujagic, M. Austerer, S. Schartner, M. Nobile, L. K. Hoffmann, W. Schrenk, G. Strasser, M. P. Semtsiv, I. Bayrakli, M. Wienold, W. T. Masselink, "Impact of doping on the performance of short-wavelength InP-based quantum-cascade lasers." Applied Physics, 103 (2008) 033104.

[6] P. G. Bolcatto, C. R. Proetto, "Shape and dielectric mismatch effects in semiconductor quantum dots." Physical Review B, 59 (1999) 12487.

[7] A. Kwasniowski, J. Adamowski, "Effect of confinement potential shape on exchange interaction in coupled quantum dots." Physics Condensed Matter, 20 (2008) 215208.

[8] M. E. M-Ramos, C. A. Duque, E. Kasapoglu, H. Sari and I. Sokmen, "Linear and nonlinear optical properties in a semiconductor quantum well under intense laser radiation: Effects of applied electromagnetic fields." Journal of Luminance, **132** (2012) 901.

[9] H. Yildirim, M. Tomak, "Third-harmonic generation in a quantum well with adjustable asymmetry under an electric field." Physics Status Solidi B, **243** (2006) 4057.

[10] S. Pal, M. Ghosh, "Tailoring nonlinear optical rectification coefficient of impurity doped quantum dots by invoking Gaussian white noise." Optical and Quantum Electronics, **48** (2016) 372.

[11] J. Ganguly, M. Ghosh, "Modulating optical second harmonic generation of impurity-doped quantum dots in presence of Gaussian white noise." Physica Status Solidi B, **253** (2016) 1093.

[12] J. Ganguly, S. Saha, A. Bera, M. Ghosh, "Modulating optical rectification, second and third harmonic generation of doped quantum dots: Interplay between hydrostatic pressure, temperature and noise." Superlattices and Microstructures, **98** (2016) 385.

[13] Y. Qiucheng, G. Kangxian, H. Meilinm, Z. Zhongmin, L. Keyin and L. Dongfeng, "Study on the optical rectification and second-harmonic generation with position-dependent mass in a quantum well." Journal of Physics and Chemistry of Solids, **119** (2018) 50.

[14] R. L. Restrepo, E. Kasapoglu, S. Sakiroglu, F. Ungan, A. L. Morales and C. A. Duque, "Second and third harmonic generation associated to infrared transitions in a Morse quantum well under applied electric and magnetic fields." Infrared Physics and Technology, **85** (2017) 147.

[15] J. C. Martínez-Orozcoa, J. G. Rojas-Briseñoa, K. A. Rodríguez-Magdalenoa, I. Rodríguez Vargasa, M. E. Mora-Ramosb, R. L. Restrepoc, F. Ungand, E. Kasapoglue and C. A. Duque, "Effect of the magnetic field on the nonlinear optical rectification and second and third harmonic generation in double δ-doped GaAs quantum wells." Physica B, **525** (2017) 30.

[16] B. Cakir, Y. Yakar, A. Ozmen, M. O. Sezer and M. Sahin, "Linear and nonlinear optical absorption coefficients and binding energy of a spherical quantum dot." Supperlattices and Microstructure, 47 (2010) 556.

[17] G. Rezaei, S. Shojaeian Kish, "Linear and nonlinear optical properties of a hydrogenic impurity confined in a two-dimensional quantum dot: Effects of hydrostatic pressure, external electric and magnetic fields." Superlattices and Microstructures, 53 (2013) 99.

[18] T. Chen, W. Xie, S. Liang, "The nonlinear optical rectification of an ellipsoidal quantum dot with impurity in the presence of an electric field." Physica E, 44 (2012) 786.

[19] S. Yilmaz, "Nonlinear Optical Rectification and Oscillator Strength in a Spherical Quantum Dot with an Off-Center Hydrogenic Impurity in Presence of an Applied Electric Field." Computational and Theoretical Nanoscience, 10 (2013) 2019.

[20] S., Shojaei, A. Soltani Vala, "Nonlinear optical rectification of hydrogenic impurity in a disk-like parabolic quantum dot: The role of applied magnetic field." Physica E, 70 (2015) 108.

[21] P. Hosseinpour, "The role of Rashba spin-orbit interaction and external fields in the thermal properties of a doped quantum dot with Gaussian impurity." Physica B: Condensed Matter, **593** (2020) 412259.

[22] M. Kauranen, A. V. Zayats, "Nonlinear plasmonics." Nature Photonics, **6** (2012) 737.

[23] C. Forestiere, A. Capretti, G. Miano, "Surface integral method for second harmonic generation in metal nanoparticles including both local-surface and nonlocal-bulk sources." JOSA B, **30** (2013) 2355.

[24] M. Sheik-Bahae, A. A. Said, T. H. Wei, D. J. Hagan, "Sensitive measurement of optical nonlinearities using a single beam." Quantum Electronics, IEEE Journal, **26** (1990) 760.

[25] I. Karabulut, U. Atav, H. Safak, "Comment on "Electric field effect on the second-order nonlinear optical properties of parabolic and semi-parabolic quantum wells."" Physical Review **B**, **72** (2005). 207301.

[26] Z. Wangjian, "A study of electric-field-induced second-harmonic generation in asymmetrical Gaussian potential quantum wells." Physica B, **454** (2014) 50.

[27] R. C. Ashoori, "Electrons in artificial atoms." Nature, **379** (1996) 413.

[28] M. A. Kastner, "Artificial Atoms." Physics Today, **46** (1993) 24.

[29] S. Shao, K. -X. Guo, Z. -H. Zhang, N. Li and C. Peng, "Studies on the second-harmonic generations in cubical quantum dots with applied electric field." Physica B, **406** (2011) 393.

[30] I. V. Martynenko, A. P. Litvin, F. P. Milton, A. V. Baranov, A. V. Fedorov and Y. K. Gunko, "Application of Semiconductor Quantum Dots in Bioimaging and Biosensing." Journal of Materials Chemistry B, **5** (2017) 6701.

[31] S. M. Reimann, M. Manninen, "Electronic structure of quantum dots." Reviews of Modern Physics, **74** (2002) 1283.

[32] N. Kumar Datta, M. Ghosh, "Oscillatory impurity potential induced dynamics of doped quantum dots: Analysis based on coupled influence of impurity coordinate and impurity influenced domain." Chemical Physics, **372** (2010) 82.

[33] G. Dresselhause, "Spin-orbit coupling effects in zinc-blends structures." Physical Review, **100** (1955) 580.

[34] E. I. Rashba, "Properties of semiconductors with an extremum loop. 1. Cyclotron and combinational resonance in a magnetic field perpendicular to the plane of the loop." Soviet Physics-Solid State, **2** (1960) 1109.

[35] N. Kumar Datta, M. Ghosh, "Impurity strength and impurity domain modulated frequency-dependent linear and second non-linear response properties of doped quantum dots." Physica Status Solidi B, **248** (2011) 1941.

[36] P. Hosseinpour, J. Barvestani, A. Soltani-Vala, "Rashba spin–orbit interaction effect on the optical properties of a disk-like quantum dot", Physica Scripta, 91 (2016) 045803.